Journal of Asian Earth Sciences 252 (2023) 105698

Contents lists available at ScienceDirect

Journal of Asian Earth Sciences

journal homepage: www.elsevier.com/locate/jseaes

Potentially important regolith-hosted Sc deposits related to alkaline igneous complexes of the Permian Emeishan large igneous Province, SW China

Wen Winston Zhao [a,b], Mei-Fu Zhou [a,b,*], Zhengchao Wang [b], Yan Hei Martin Li [b], Liang Qi [b], Wei Terry Chen [b], Yu Shen [b]

[a] School of Earth Resources, China University of Geosciences, Wuhan 430074, China
[b] State Key Laboratory of Ore Deposit Geochemistry, Institute of Geochemistry, Chinese Academy of Sciences, Guiyang 550081, China

ARTICLE INFO

Keywords:
Scandium
Regolith
Alkaline complex
Exploration
SW China

ABSTRACT

Scandium (Sc) is one of several important critical metals with increasing applications in modern industry. However, Sc is highly dispersed in nature and is rarely sufficiently concentrated to form Sc-dominated deposits. Therefore, finding new Sc resources is now urgently needed to ensure future sustainable supplies. We report, for the first time, the potential Sc resources in regolith developed over pyroxenites of the Jijie and Shuikoujing alkaline complexes of the Permian Emeishan Large Igneous Province (ELIP), SW China. The weathering profiles are variable, but typically consist of soft pedolith in the upper part and solid saprolith in the lower part. Overall, the pedolith and saprolith in Jijie and Shuikoujing have average Sc grades of 83.2 ppm to 91.5 ppm and 57.4 ppm to 58.3 ppm, respectively, which are two- to five-fold those of fresh bedrocks. There are abundant pyroxene relicts in both the pedolith and saprolith. Scandium is mainly hosted in montmorillonite and goethite, which may be much easier and more suitable for mining than the bedrock. At the early stage of weathering, Sc concentrations correlate positively with the abundances of secondary montmorillonite. The highest Sc concentration coincides with the appearance of goethite which is the major host of Sc during the late stage of weathering. However, Sc is depleted in the transition zone between the saprolith and pedolith, which might be ascribed to the absence of both montmorillonite and/or goethite. Our preliminary study estimates ~1,100 to ~3,500 tonnes of Sc metal in the regolith developed above the two alkaline complexes. With the increasing market interest and improvements in recovery methods, these Sc resources in Jijie and Shuikoujing can be considered potentially important Sc deposits.

1. Introduction

Scandium (Sc) is one of several critical metals with broad applications and plays a pivotal role in modern advanced technologies. For example, it can be used as a doping agent to strengthen aluminum alloys for the aerospace and automobile industries, and is used in solid oxide fuel cells to improve conductivity and lower the operating temperature (Voncken, 2016). However, Sc is highly dispersed in nature and is currently produced exclusively as by-product of other ore deposits. In the world, Sc annual production is less than 25 tonnes (USGS, 2021). Currently, it is mainly sourced from tailings of the Bayan Obo REE deposit, China, but other sources include wolframite, pegmatites, red mud, and coal waste (Williams-Jones and Vasyukova, 2018; Wang et al., 2021; Liu et al., 2023). The gap between demand and supply of Sc is predicted to increase over the next decade, and thus, it is urgent to find new resources to ensure future sustainable supplies.

Scandium can be greatly enriched in regolith developed over various types of rocks, showing that such deposits are potential Sc resource (e.g., Aiglsperger et al., 2016; Maulana et al., 2016; Chassé et al., 2017; Putzolu et al., 2019; Teitler et al., 2019; Ulrich et al., 2019). Regolith-hosted Sc deposits have been reported over pyroxenite of Alaskan-type mafic–ultramafic rocks (e.g., Chassé et al., 2019; Putzolu et al., 2019), as well as peridotite (e.g., Teitler et al., 2019; Ulrich et al., 2019), basalt (e.g., Sun et al., 2021), and granitoids (e.g, Wang et al., 2010; Zhao et al., 2012; Shen, 2002). However, Sc contents in most regoliths are relatively low, and would rarely qualify as economically attractive, standalone

* Corresponding author.
E-mail address: zhoumeifu@hotmail.com (M.-F. Zhou).

https://doi.org/10.1016/j.jseaes.2023.105698
Received 31 December 2022; Received in revised form 23 April 2023; Accepted 25 April 2023
Available online 1 May 2023

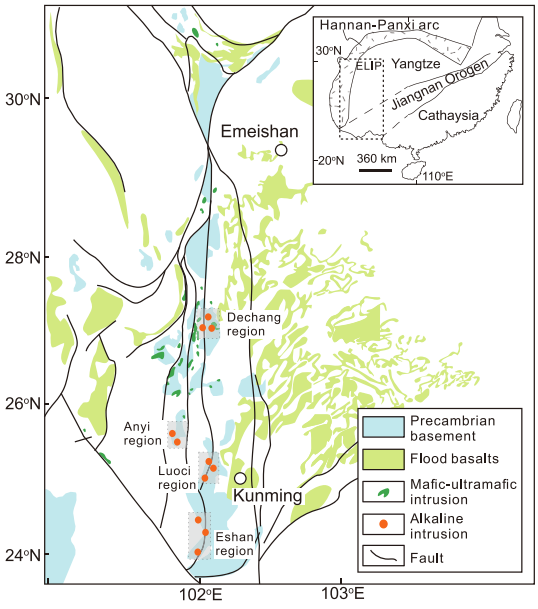

Fig. 1. Simplified geological map showing the location of ELIP, SW China, and distribution of continental flood basalts and various mafic–ultramafic intrusions (modified after Zhou et al. (2022) and references therein).

resources, but could be sufficient as a highly valuable by-product (Orberger and van der Ent, 2019; Zhou et al., 2020). On the other hand, some regolith developed over Alaskan-type pyroxenites do contain relatively high Sc concentrations. For instance, an exceptionally high Sc concentration (434 ppm) has been recognized in the laterite developed over clinopyroxenite in the Syerston-Flemington deposits in Eastern Australia, which make it potentially minable (Chassé et al., 2017; 2019). Recently, Zhou et al. (2022) reported significant Sc-enrichment of pyroxenites in alkaline complexes of the ca. 260 Ma ELIP, SW China, and proposed that they are potentially important deposits as low-grade ores with large tonnages. Our preliminary studies show that weathering profiles are well developed over these alkaline complexes, but systematic vertical sampling of complete profiles was lacking. Therefore, the significance of Sc concentrations in those regoliths were poorly constrained.

In this study, we systematically sampled weathering profiles in the Jijie and Shuikoujing alkaline complexes through drilling by a soil auger and a backpack rotary drill. Using major and trace elemental data and X-ray diffraction (XRD) results for the different parts of the sampled regoliths, we assessed the possibility using regoliths as a Sc-dominated resource and conclude that the alkaline igneous complexes of the ELIP are potentially important Sc deposits. Such sources would reduce the dependence of Sc supplies from the limited known deposits and help ensure a potentially sustainable and reliable supply.

2. Geological background

2.1. Reginal geology

The South China Block is composed of the Yangtze Block in the north and Cathaysia Block in the south, which are separated by the Jiangnan Orogen (Fig. 1). The Yangtze Block has an Archean to Paleoproterozoic basement, which is unconformably overlain by Neoproterozoic and Sinian sedimentary successions and a Phanerozoic cover sequence of limestone, dolomite, conglomerate, sandstone, and black shale (Zhao and Cawood, 2012; Wang et al., 2013). Along the western and northern margins of the Yangtze Block, Neoproterozoic mafic–ultramafic intrusions and granitic plutons form the Hannan-Panxi arc, which may

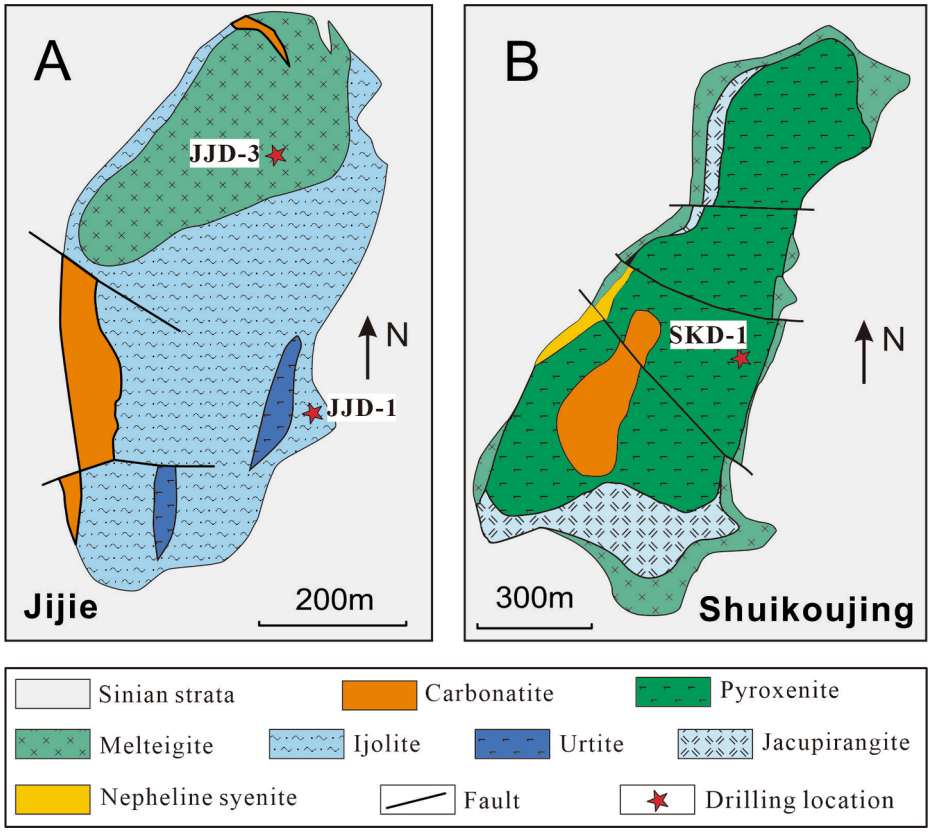

Fig. 2. Geological map of the Jijie (A) and Shuikoujing (B) intrusions (modified after Zhou et al. (2022) and references therein). Drilling locations are denoted by red stars. (For interpretation of the references to colour in this figure legend, the reader is referred to the web version of this article.)

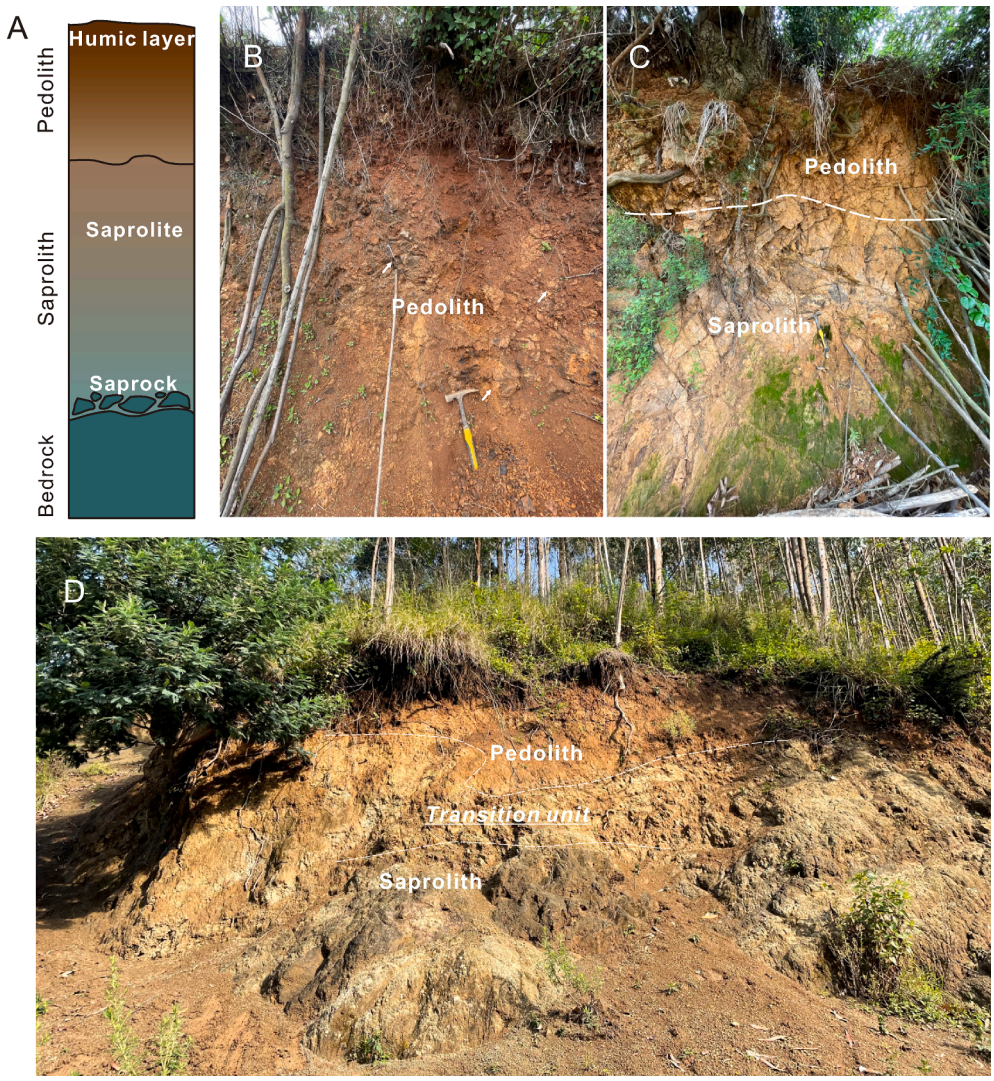

Fig. 3. Cartoon showing typical regolith profile (A). Field photos of the regolith developed after alkaline complexes in Jijie (B-C) and Shuikoujing (D).

relate to the Neoproterozoic subduction of oceanic crust (Zhou et al., 2002a). Late Mesoproterzoic and early Neoproterozoic metamorphosed volcanic-sedimentary strata are widespread in both the Jiangnan Orogen and the Hannan-Panxi arc.

The ELIP is exposed in the western part of the Yangtze Block (Fig. 1). Widespread continental flood basalts extend from eastern Tibet to northwestern Vietnam (Chung and Jahn, 1995). The volcanic sequence in the ELIP is composed of picrites, basalts, basaltic andesites, and rhyolites (Chung and Jahn, 1995, Xu et al., 2004) along with small quantities of alkaline volcanic rocks (Mei et al., 2003). The thickness of the volcanic succession is highly variable from several hundred meters in the east to ~5 km in the west, which is probably due to post-eruption tectonic activity leading to strong uplift and erosion in the Mesozoic and Cenozoic (Xu et al. 2004; Ali et al., 2005; Liu et al. 2020). Plutonic rocks in the ELIP, including mafic–ultramafic intrusions, are mostly exposed along major N-S trending faults, which host some world-famous, giant magmatic Cu–Ni–sulfide and Fe–Ti–(V) oxide deposits (Ma et al., 2003; Song et al. 2003; Wang et al. 2007; Zhou et al., 2005; Zhong et al. 2011). These Ni-Cu-sulfide and oxide-bearing intrusions were mostly emplaced at around 260 Ma and were related to the plume-derived magmas (Zhou et al., 2002b; Shellnutt et al., 2008, 2012).

2.2. *Alkaline igneous complexes of the ELIP*

Several alkaline igneous complexes are distributed in the ELIP from the south to north, mainly in the Eshan, Luoci, Anyi and Dechang regions (Fig. 1) (Zhou et al., 2022). These complexes are zoned and were originally thought to be Alaskan-type bodies (Cao et al. 1993; Zhu, 2010; Guo et al. 2012). Recent studies show that these intrusions have distinct bulk-rock compositions and mineralogical geochemistry (Wang et al., 2022; Zhou et al., 2022). Several geochronological studies demonstrate that these complexes emplaced between 248 and 260 Ma and are part of the ELIP (e.g., Wang et al., 2022).

The Jijie and Shuikoujing intrusions in the Luoci region are two of the most typical alkaline igneous complexes in the ELIP (Fig. 2). They are mainly composed of pyroxenite, jacupirangite, meleigite, ijolite, urtite, and nepheline syenite. Zhou et al. (2022) reported for the first time that these complexes are mostly composed of clinopyroxene with variable amounts of apatite and magnetite and have 39 to 71 ppm Sc, which may be high enough to justify mining under the current Sc prices.

2.2.1. *Jijie complex*

The Jijie complex is elliptical in shape with an exposed area of about 0.29 km^2 (Fig. 2A). The zoned complex is composed of ijolite and melteigite from the rim to the core, and is intruded by urtite and nepheline syenite. The complex may also contain some carbonatites, but their

Fig. 4. Field photos of the drilling techniques and core samples of different parts of regolith profile. (A) Sampling by the soil auger. (B) Sampling by the backpack rotary drill. (C) Top humic layer samples. (D) Typical pedolith samples. (E) Saprolite samples. (F) Saprock samples.

origin should be further studied. The ijolite has an intrusive contact with fine-grained melteigite, which is mainly composed of euhedral and subhedral aegirine (60–75%) that mostly forms green, columnar crystals, and subhedral nepheline (15–30%) with minor apatite, olivine, magnetite, and biotite (~10% in total). Zoning is ubiquitous in the aegirine grains with higher MgO in the cores and FeO in the rims.

2.2.2. Shuikoujing complex

The Shuikoujing complex is about 1470 m long and up to 830 m wide, with an exposed area of about 0.69 km^2 (Fig. 2B). The intrusion is funnel-shaped in three dimensions as revealed by drilling. The Shuikoujing complex is composed of melteigite, jacupirangite, and pyroxenite from the rim to the core. A newly-identified carbonatite outcrops in the southwestern part of the complex on the top of Shuikoujing mountain. The pyroxenite occupies most of the complex with an exposed area of ~0.35 km^2. Euhedral to subhedral clinopyroxene crystals make up 70–90% of the pyroxenite, accompanied by amphibole, plagioclase, Fe-Ti oxides, and minor apatite.

3. Weathered profiles of the Jijie and Shuikoujing alkaline complexes

Regoliths associated with the Jijie and Shuikoujing intrusions are both developed on highly heterogeneous bedrocks. In profile, the regolith is generally layered from a pedolith zone in the upper part, downward through a saprolith zone, to a bedrock of parent rock (Fig. 3A). In general, the pedolith is red-brown or brownish yellow, and made up of mottled and/or ferruginous layers overlain by an upper humic layer. The pedolith layer is commonly developed in situ but can also contain transported materials. In the pedolith, the original bedrock structure has been destroyed by weathering of the original minerals and the redistribution of secondary materials such as clays and oxides. In some cases, remnants of primary minerals or weathered rock fragments may remain in the fine-grained matrix, composed of a mixture of Fe oxides and oxyhydroxides (Fig. 3B). The pedolith has important interstitial porosity with fractures, which are usually filled by a black fine-grained matrix, mostly Mn oxides, or by a white homogeneous matrix, mostly calcite. The saprolith beneath the pedolith retains the original bedrock structures, but the bedrock fabric is mostly weathered (Fig. 3C). Generally, the saprolith consists of saprolite and saprock. The saprock in the lower part generally resembles the bedrock, preserving most of its primary mineralogy and texture, although the primary minerals have been partially replaced along cleavages. The weathering intensity is largely controlled by the joint density with strong staining and discoloration of saprock evident in the well-jointed intervals. The saprolite is medium- to fine-grained, and dominated by clay minerals, particularly smectite, with accessory remnants of minerals identified mostly as pyroxenes, and minor rust-colored areas formed by weathered crystals covered by Fe oxides. The unit transitions upward into the pedolith, which is light brown to pale yellow (Fig. 3D). The thickness of this unit is variable, and porosity gradually increase upward where pre-existing structures may have collapsed.

4. Analytical methods

4.1. Sampling strategy and petrographic observations

Regolith samples were sampled on the surface and by drillings. Surface samples were randomly collected in Shuikoujing, Jijie, and Zhushidian complexes of the Luoci region, and Yuhezhai and Dalongtan complexes of the Eshan region. Three holes were drilled in the regoliths overlying melteigite and ijolite in the Jijie intrusion and pyroxenite in Shuikoujing body (Fig. 2), which are main phases in the alkaline complexes (Zhou et al., 2022). The soft parts of the regolith profiles were obtained using a 10-cm-diameter soil auger, and the solid parts were sampled with a backpack rotary drill with a 2-cm-diameter bit (Fig. 4).

Air-dried, resin-impregnated polished thin sections were prepared for both intact samples and broken chips. Petrographic observations were made using an optical microscope and a scanning electron microscope equipped with secondary electron (SE) and backscatter electron (BSE) detectors to examine both surface morphologies and differences in chemistry, and an Oxford INCAx-sight energy-dispersive spectrometer for mineral identification (Fig. 5).

4.2. X-ray diffraction

The major minerals were identified and their abundances determined using quantitative XRD analyses. Samples were ground to a fine powder using an agate mortar and pestle and analyzed at the State Key Laboratory of Ore Deposit Geochemistry, Institute of Geochemistry of Chinese Academy of Sciences (IGCAS), Guiyang, with a D8 Focus Bruker powder X-ray diffractometer. Each sample was X-rayed with non-monochromatic Cu Kα radiation (40 kV, 40 mA) from 2° to 70° 2θ at a scanning speed of 2°/min. The diffractograms were analyzed and the proportions of the different minerals determined through a Rietveld refinement using the JADE 6.5 software.

4.3. Bulk rock geochemistry

Bulk rock element contents were measured using inductively coupled plasma optical emission spectrometry (ICP-OES) and/or X-ray fluorescence (XRF) for major oxides, and inductively coupled plasma mass spectrometry (ICP-MS) for trace elements, at both the Australian Laboratory Service (ALS) P/L and the State Key Laboratory of Ore Deposit Geochemistry, IGCAS (Qi et al., 2000). Analytical precisions for both ALS and IGCAS are < 1 % for major oxides and < 5 % for trace elements.

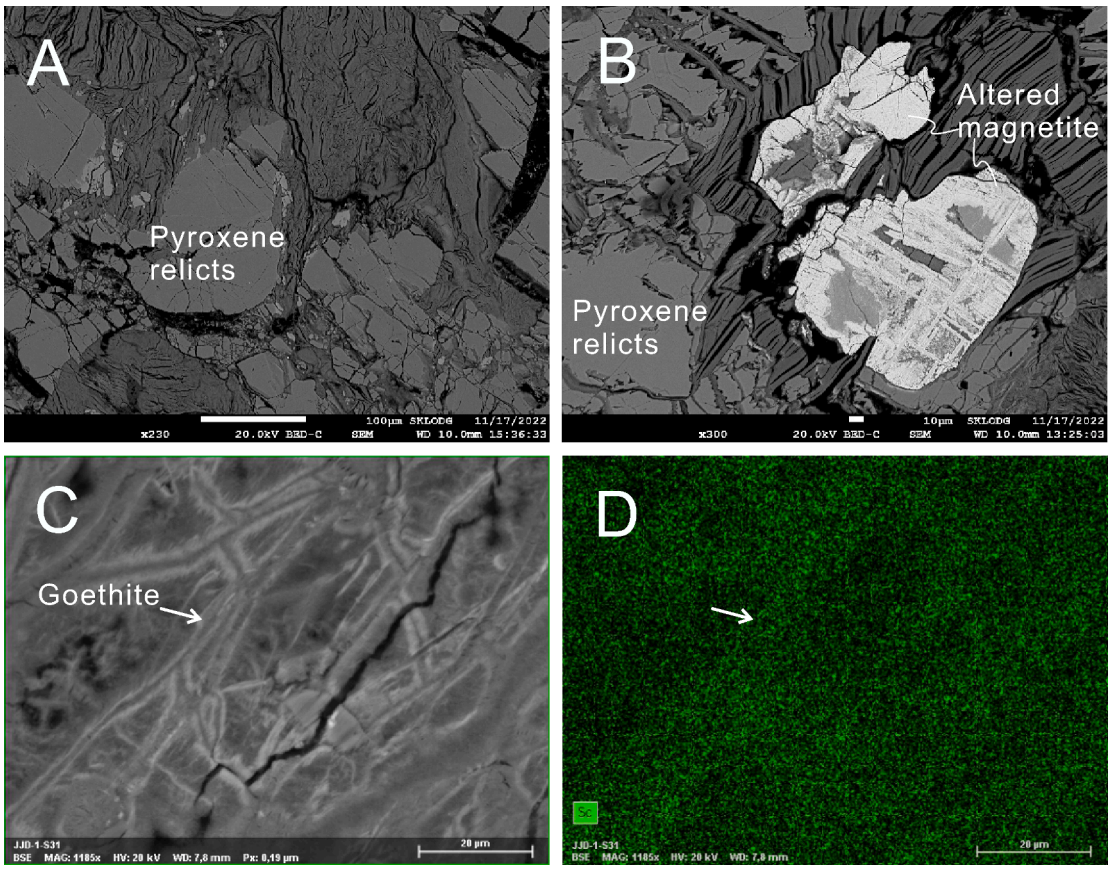

Fig. 5. Back scattered images showing the mineralogy (A-C) in pedolith and saprolith from the Jijie and Shuikoujing regolith profiles, and EDS Sc mapping of C (D).

Table 1
Summary of major elemental oxides, loss on ignition (LOI), and index of lateritisation (IOL) of regolith samples from the Shuikoujing and Jijie complexes, SW China.

	Shuikoujing			Jijie		
	Average	Maximum	Minimum	Average	Maximum	Minimum
SiO_2* (wt%)	46.28	50.84	42.05	30.00	39.40	22.60
TiO_2 (wt%)	1.42	2.33	0.80	5.70	9.80	3.50
Al_2O_3 (wt%)	8.84	14.74	4.74	13.70	22.10	5.70
TFe2O3 (wt%)	9.74	14.50	5.78	32.70	50.90	19.60
MnO (wt%)	0.14	0.21	0.10	0.41	0.73	0.26
MgO (wt%)	11.02	14.45	5.33	2.96	10.53	0.40
CaO (wt%)	16.19	25.24	7.78	2.95	14.87	0.12
Na_2O (wt%)	0.99	2.00	0.50	0.13	1.21	0.01
K_2O (wt%)	0.27	1.98	0.00	0.21	0.85	0.06
P_2O_5 (wt%)	0.15	0.44	0.03	0.81	5.18	0.11
LOI (wt%)	4.95	10.83	1.72	10.43	15.58	2.06
IOL	–	39.71	17.93	–	71.70	41.90

Note: *Values calculated by: SiO_2 = 100-(LOI + other major oxides); "-" means values not available or below 0.01.

5. Analytical results

5.1. Major oxides and Sc concentrations

Major and trace elemental contents of regolith samples from the Jijie and Shuikoujing complexes are summarized in Table 1. Regolith samples in Jijie have SiO_2 contents from 22.6 to 39.9 wt%, and $Na_2O + K_2O$ contents of 0.07 to 2.1 wt%, which are all typically lower than those of melteigite-ijolite (SiO_2: 38.9–43.6 wt%; $Na_2O + K_2O$: 4.8–13.7 wt%; Zhou et al., 2022). In contrast, the regolith samples have TiO_2 contents of 2.9–9.9 wt%, TFe_2O_3 contents of 14.8–50.9 wt%, Al_2O_3 contents of 5.3–22.1 wt%, which are all obviously higher than those of melteigite-ijolite (TiO_2: 1.8–2.8 wt%; TFe_2O_3: 10.8–18.1 wt%; Al_2O_3: 9.1–17.5 wt%; Zhou et al., 2022). However, major oxides of the Shuikoujing regolith samples are very similar to those of the fresh bedrock. Generally, they have SiO_2 contents of 42.1 to 50.8 wt%, and $Na_2O + K_2O$ contents of 0.54–3.0 wt%, TiO_2 contents of 0.8 to 2.3 wt%, TFe_2O_3 contents of 5.8 to 14.5 wt%, and Al_2O_3 contents of 4.7 to 14.7 wt%, which are similar to those of the pyroxenite (SiO_2: 35.3–44.6 wt%; $Na_2O + K_2O$: 0.8–5.5 wt%; TiO_2: 1.4–3.5 wt%; TFe_2O_3: 9.1–25.9 wt%; Al_2O_3: 6.7–13.0 wt%; Zhou et al., 2022) and jacupirangite-melteigite (SiO_2: 39.8–45.5 wt%; $Na_2O + K_2O$: 4.1–5.4 wt%; TiO_2: 1.1–2.3 wt%; TFe_2O_3: 10.9–19.1 wt%; Al_2O_3: 9.7–16.1 wt%; Zhou et al., 2022).

Regolith samples in this study show variable Sc concentrations (Table 2). In the Shuikoujing regolith, Sc contents range from 41 ppm to 114 ppm, with average Sc concentrations of 92 ppm in the pedolith and 57 ppm in the saprolith. Similarly, in the Jijie regolith, Sc contents range from 43 ppm to 142 ppm, with average Sc concentrations of 83 ppm in

Table 2
Summary of Sc concentrations of regolith and bedrock from the Shuikoujing and Jijie complexes and other complexes in ELIP, SW China.

		Sc		
		Average	Maximum	Minimum
Shuikoujing	Pedolith (n = 69)	92	114	51
	Saprolith (n = 28)	57	81	41
	Pyroxenite*	56	71	45
	Melteigite*	33	44	23
	Jacupirangite*	43	47	22
Jijie	Pedolith (n = 92)	83	142	36
	Saprolith (n = 17)	58	71	43
	Melteigite*	40	53	25
	Ijolite*	30	42	16
Zhushidian	Regolith (n = 4)	40	51	34
Yuhezhai	Regolith (n = 80)	41	67	20
Dalongtan	Regolith (n = 20)	37	54	17

Note: * Data from Zhou et al. (2022) and reference therein.

the pedolith and 58 ppm in the saprolith. The major phases of Shuikoujing complex (pyroxenite, melteigite, and jacupirangite) and Jijie complex (melteigite and ijolite) have Sc contents of 22–71 ppm and 16–53 ppm, respectively (Zhou et al., 2022). As such, it is obvious that regolith samples in Shuikoujing and Jijie generally contain two- to five-fold of Sc than those of the fresh bedrocks (Fig. 6A and B). We also note that in Jijie, TiO_2 contents are two- to four-times higher than the bedrocks, and show positive correlations with Sc concentrations but such trends are not clear in Shuikoujing. Comparatively, regolith samples from the Zhushidian, Yuhezhai, and Dalongtan complexes have lower average Sc concentrations of 40 ppm, 41 ppm, and 37 ppm.

The loss on ignition (LOI) in the regoliths is proportional to the abundance of hydrated minerals, such as clay minerals. Regolith samples from Jijie and Shuikoujing, both have highly variable LOI values of

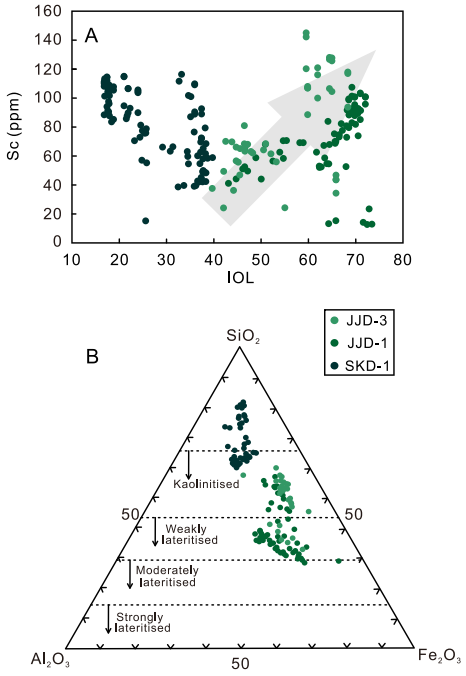

Fig. 7. Plots of Sc concentrations and IOL (A). SAF diagram (B).

2.1 to 15.6 wt% and 1.7 to 10.8 wt%, respectively, which may imply different degree of weathering (e.g., Duzgoren-Aydin and Aydin, 2003). Shuikoujing regolith samples have obviously higher LOI values than the fresh bedrock, but Sc concentrations do not show a clear relationship with LOI values (Fig. 6C). In Jijie, regolith samples also have clearly

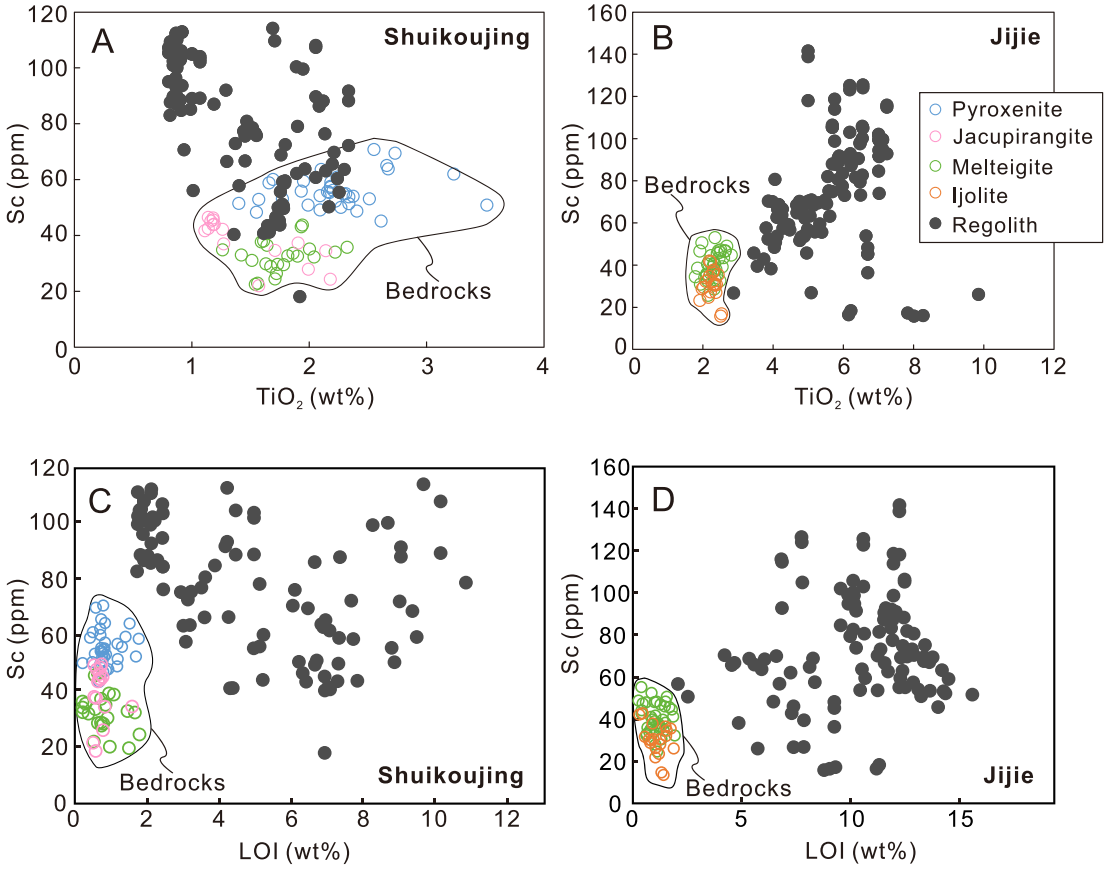

Fig. 6. Binary diagrams showing the relationships between Sc concentrations and TiO_2 contents (A-B), and LOI (C-D).

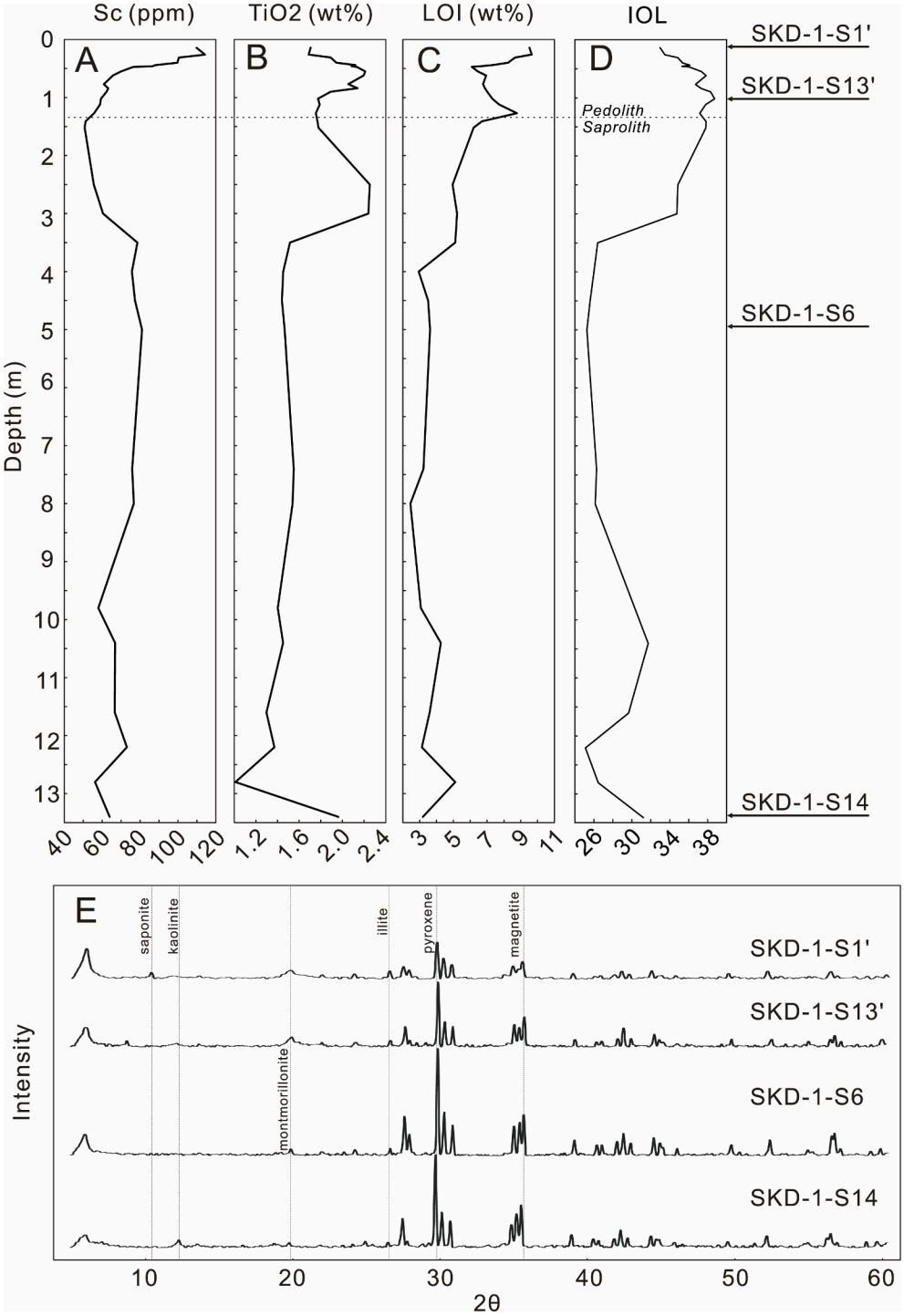

Fig. 8. Sc, TiO_2, LOI, IOL variations (A-D), and XRD results of representative samples (E) from the SKD-1 regolith profile developed after the Shuikoujing alkaline complexes.

higher LOI values than those of fresh bedrocks, and Sc concentrations shows roughly positive trends with the LOI values (Fig. 6D).

The index of laterization (IOL) was used to quantify the stages of advanced chemical weathering, and higher IOL values correspond to more intensely weathered samples, which are characterized by the formation of gibbsite, goethite and hematite (Kisakürek et al., 2004). The IOL is calculated by the mass (wt%) ratio of SiO_2, TFe_2O_3, and Al_2O_3 ($IOL = 100*[(Al_2O_3 + TFe_2O_3)/(SiO_2 + Al_2O_3 + TFe_2O_3)]$) (Babechuk et al., 2014). Accordingly, regolith samples from Jijie have IOL values ranging from 39.7 to 71.7, and those from Shuikoujing have IOL from 17.9 to 39.7. This implies that regolith samples from Shuikoujing could be much less weathered than those from Jijie. Sc concentrations of samples in Jijie show roughly positive correlations with IOL, whereas samples from Shuikoujing do not have such a relationship (Fig. 7A). Similarly, In the SiO_2-Al_2O_3-TFe_2O_3 (SAF) ternary plots proposed by Schellmann (1986), regolith samples from Shuikoujing plot near the boundary of kaolinitsed weathering residues, representing early stages of weathering, whereas samples from Jijie all plot in the fields of kaolinitised and lateritised weathering residues representing intermediate- to late-stages of weathering (Fig. 7B).

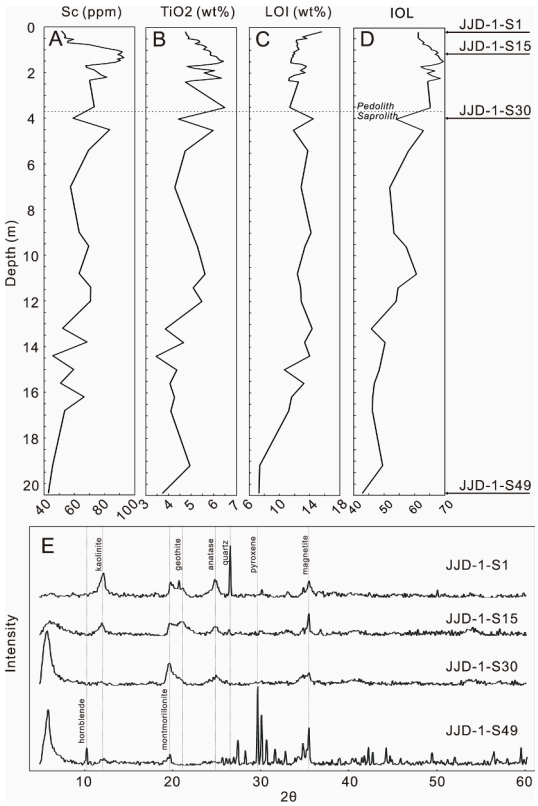

Fig. 9. Sc, TiO_2, LOI, IOL variations (A-D), and XRD results of representative samples (E) from the JJD-1 regolith profile developed after the Jijie alkaline complexes.

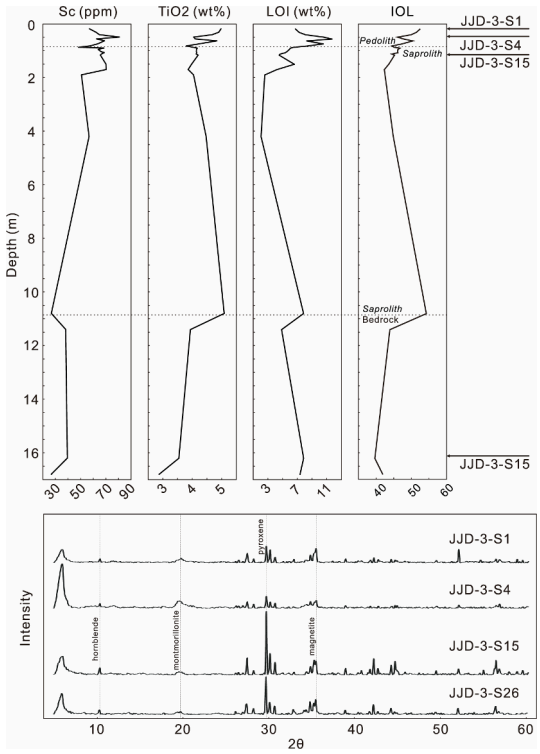

Fig. 10. Sc, TiO2, LOI, IOL variations (A-D), and XRD results of representative samples (E) from the JJD-3 regolith profile developed after the Jijie alkaline complexes.

5.2. Sc concentrations and mineralogical variations through profiles

In drill hole SKD-1, Sc is enriched in the top layer of the Shuikoujing pedolith profile, where Sc contents can be up to more than 100 ppm, twice those of fresh bedrocks. Then, Sc contents gradually decline to ~51 ppm towards the bottom of the pedolith, a change accompanied by a transition from brown to pale yellow colors. The top of saprolith has Sc contents up to ~81 ppm, similar to those at the bottom of the pedolith and then decline downward. Overall, the pedolith has Sc contents of 55.7 to 114 ppm, and the saprolith has Sc contents of 50.8 to 81.0 ppm. In drillhole SKD-1, which penetrated the pedolith and the transition unit, IOL values are higher than those of the saprolith, and LOI values are relatively low, decreasing gradually from the transition unit to the top of the pedolith. Montmorillonite is more common in the pedolith samples, and in drillhole SKD-1-S1′, it is joined by saponite, another smectite group mineral. Pyroxene and magnetite are present in all samples from saprolith to pedolith, but appears to be less abundant in the pedolith than in the saprolith (Fig. 8).

In the drill hole JJD-1 of the Jijie intrusion, the pedolith has Sc contents from 51.6 to 92.8 ppm, and the saprolith has values of 42.9 to 83.4 ppm, mostly between depths of 0.7 to 3.5 m. The top of the saprolith has lower Sc contents of ~60 ppm, which decrease downward to 50 ppm in the saprock at a depth of 20 m. TiO_2 contents are higher in the pedolith and saprolith, consistent with the appearance of anatase. The LOI values are higher in the saprolith than the pedolith, corresponding to an increase in the abundance of montmorillonite. The IOL values increase from the saprolith to pedolith, and the highest IOL values correlate with the high Sc concentrations in the pedolith, which may reflect the presence of goethite (Fig. 9). The top layers of JJD-1 have some quartz, which may imply that these layers were contaminated by other sources.

In drill hole JJD-3, the pedolith has Sc concentrations from 56.9 ppm to 80.6 ppm, and is most enriched in the middle layers of the pedolith below the humic layers. The saprolith has Sc contents of 50.6 to 70.3 ppm, with the lower values at the transition from saprolith to pedolith. Sc contents then remain at ~50 ppm down to 4 m, an interval of saprock above the fresh parent rocks. From 10 m downwards, fresh bedrock has Sc contents ranging from 26.7 to 39.5 ppm. TiO_2 contents are also remarkable high in the pedolith, which also has LOI and IOL values. Montmorillonite zones in the pedolith have relatively high Sc concentrations. However, pyroxene grains are present in all samples of the pedolith but its abundance correlates inversely with Sc concentrations (JJD-3-S4) and the abundance of montmorillonite. Magnetite is significant in all samples, but anatase is absent (Fig. 10).

6. Mechanism of Sc concentration via weathering of alkaline complexes

Scandium has a much smaller radius (0.87 Å) than other rare earth elements (REEs) (1.16–0.97 Å) (Shannon, 1976), and thus is not typically associated with REE deposits (Williams-Jones and Vasyukova, 2018; Wang et al., 2021; Liu et al., 2023). Notably, Sc has a close affinity with Fe, Mg, and high field strength elements (HFSE) such as Nb, Ta, Ti, W, and Sn (e.g., Dill et al., 2006; Kempe and Wolf, 2006). Therefore, in the protolith, mafic minerals, particularly pyroxene and amphibole, and some HFSE-rich minerals such as baddeleyite, zirconolite, columbite, ilmenite, wolframite, and cassiterite, can have high abundances of Sc. In the Jijie and Shuikoujing intrusions, pyroxene is the most common and abundant mineral in the protolith (Fig. 5). It has high Sc concentrations, which may be due to the much higher partition coefficient of Sc between pyroxene and alkaline mafic magmas compared to tholeiitic magmas (Wang et al. 2022; Zhou et al., 2022).

During weathering process, Sc is proposed to be released from the parent rocks and incorporated in secondary smectite group minerals and then further concentrated when the smectite dissolves and the Sc is re-absorbed in goethite (Chassé et al., 2019). In the ELIP alkaline intrusions, the saprolite and saprock of saprolith record the first stages of

Table 3
Exploration Target range estimation for regolith-hosted Sc resources of the Shuikoujing and Jijie complexes, SW China.

		Exploration Target: Estimated Sc Grade[1] (ppm)		Exploration Target: Estimated Volume[2] (km3)		Exploration Target: Estimated Tonnage[3] (million tonnes)		Exploration Target: Estimated Sc Mineralization Potential[4] (tonnes)	
		from	to	from	to	from	to	from	to
Shuikoujing	Pedolith	64.1	119.0	0.001	0.003	1.1	4.6	73	542
	Saprolith	40.2	74.6	0.006	0.009	15.2	22.8	610	1,699
Jijie	Pedolith	58.2	108.1	0.001	0.002	1.4	2.9	84	310
	Saprolith	40.8	75.8	0.004	0.005	8.8	12.0	358	907
Total Exploration Target								**1,125**	**3,458**

Note:
1 The Sc grade estimates for all Exploration Target was based on the average grade (+/-30%) of available geochemical analyses of published literature and this study.
2 The surface area of Exploration Target is quantitatively measured on geological map. Down-dip Exploration Target range is qualitatively estimated to be 3–6 m of pedolith and 11–15 m of saprolith in Jijie and 1–4 m of pedolith and 8–12 m of saprolith in Shuikoujing based on field reconnaissance.
3 The estimated potentially mineralized Exploration Target is assumed to have similar density of 1.5 g/cm^3 for pedolith and 2.5 g/cm^3 for saprolith.
4 It is important to note that the Exploration Target statement contains quantity and grade estimations that are conceptual in nature. To date there has been insufficient exploration to estimate a Mineral Resource, and it is uncertain if further exploration will result in the estimation of a Mineral Resource.

alteration of the pyroxenite, leading to the formation of smectite, including montmorillonite and/or saponite, and minor amount of Fe oxyhydroxides. At this stage, Sc was released from pyroxene and likely incorporated into the smectite, as indicated by the positive correlation between the smectite abundance and Sc concentrations in the profiles (Figs. 8-10). Therefore, as shown in the Jijie and Shuikoujing intrusions, the SKD-1 and JJD-3 regolith profiles were not completely weathered, leaving abundant pyroxene relicts (Figs. 8 and 10), indicating an early stage of weathering modification. Accordingly, the Sc concentrations in these profiles are mainly controlled by the abundance of secondary montmorillonite and pyroxene relicts. In the completely-weathered JJD-1 regolith profile, the highest Sc concentration is accompanied with the appearance of goethite (Fig. 9), implying that goethite is a major host of Sc during the further weathering, an observation that is supported by our EDS mapping (Fig. 5).

Supergene processes under tropical and sub-tropical climates can concentrate Sc through weathering of protoliths to form regolith-hosted ore deposits. The intensity of chemical weathering is significantly controlled by climate, especially the annual precipitation (e.g,. White, 1995). The Jijie and Shuikoujing intrusions are exposed to a warm subtropical climate. In this region, mean annual air temperature is 14.6 °C, and mean annual precipitation is 985 mm, resulting in the less-lateritized red soils (Ji et al., 2004) (Fig. 7B). Such weak lateritization may partially result in the relatively low Sc concentrations in the Jijie and Shuikoujing regolith, compared to the completely lateritized regolith profile in Eastern Australia (Chassé et al., 2017).

7. Tonnage of Sc metal and exploration in alkaline complexes

To date the global supply and consumption of Sc are similar and estimated to be about 20 to 25 tonnes per year, mainly in the use of Al-Sc alloys and solid oxide fuel cells (Wang et al., 2021). Sc is almost exclusively recovered as a by-product from residues, tailings and waste liquors in production of other metals (Wang et al., 2011), but recent discoveries of unusually high-grade lateritic Sc ores in Eastern Australia (up to 434 ppm Sc) would make it potentially mined as a primary product (Chassé et al., 2017; Jaireth et al., 2014). Our early study shows that alkaline complexes in Jijie and Shuikoujing have moderate Sc concentrations of 39–71 ppm, and are potentially low-grade Sc resources (Zhou et al., 2022). Although the Sc concentrations in the regoliths are two- to five-fold higher than those of bedrocks, such high concentrations that could be compared to those in Australia are not observed in the Jijie and Shuikoujing intrusions. With a maximum Sc of ~140 ppm and average values of 83.2–91.5 ppm in the pedoliths and 58.3–57.4 ppm in the saproliths (Table 2), the Sc contents in the Jijie and Shuikoujing regoliths are much more comparable to those in New Caledonia, Cuba, Dominican Republic and Indonesia (Aiglsperger et al., 2016; Maulana et al., 2016; Ulrich et al., 2019). At these grades, Sc may be valuable as a by-product, and thus the potential of Sc production in Jijie and Shuikoujing is limited for the present. However, the notable Ti contents in Jijie and probably Shuikoujing, could be also a potential recoverable resource with Sc, combined with recent improvements on recovery methods, the regoliths in Jijie and Shuikoujing could be worth considering as mineable Sc deposits in the future.

In view of its potential importance, we conduct the Exploration Target estimates of Sc resources for the pedoliths and saproliths in the Jijie and Shuikoujing complexes which are reported in compliance with the JORC Code 2012 Edition. The purpose of these estimates is to highlight potential resources for further exploration and exploitation. Scandium grades for Exploration Targets are based on average grades (+/-30%) of available geochemical analyses of regolith in Jijie and Shuikoujing. Down-dip of the Exploration Targets is qualitatively estimated to be 3 to 6 m of pedolith and 11 to 15 m of saprolith in Jijie, and 1 to 4 m of pedolith and 8 to 12 m of saprolith in Shuikoujing based on preliminary drilling results and field reconnaissance. The surface areas of the Exploration Targets have been measured from available geological maps, and 10% of the areas were added to reveal the slope. The estimated potentially mineralized Exploration Targets are assumed to have a density of 1.5 g/cm^3 for pedolith and 2.5 g/cm^3 for saprolith. Our estimates reveal a Sc mineralization potential of ~1100 to ~3500 tonnes for the Exploration Targets of the regolith of the Shuikoujing and Jijie complexes (Table 3). It is important to note that the Exploration Target statement contains quantity and grade estimations that are conceptual in nature. To date there has been insufficient exploration to allow accurate estimates for a Sc Mineral Resource, and it is uncertain if further exploration will produce results that are consistent with our estimates.

8. Conclusions

The pedolith and saprolith covering the Jijie and Shuikoujing alkaline complexes of the ELIP have average Sc grades of 83.2 ppm to 91.5 ppm and 57.4 ppm to 58.3 ppm, respectively, which are two- to five-fold of those of fresh bedrocks. The estimated resources are ~1100 to ~3500 tonnes of Sc in the regolith as the Exploration Target. The Sc grades of the Jijie and Shuikoujing regoliths are comparable to those in New Caledonia, Cuba, Dominican Republic and Indonesia. In the regolith, Sc is mainly hosted in the smectite and goethite, which may be easy for mining and exploitation. With the increasing market interest and improvements in recovery methods, it could be worth considering Sc as a future resource in the regoliths of the Jijie and Shuikoujing intrusions.

CRediT authorship contribution statement

Wen Winston Zhao: Investigation, Visualization, Writing – original draft, Writing – review & editing. **Mei-Fu Zhou:** Supervision, Conceptualization, Investigation, Visualization, Writing – original draft, Writing – review & editing. **Zhengchao Wang:** Investigation, Visualization, Writing – original draft, Writing – review & editing. **Yan Hei Martin Li:** Writing – review & editing. **Liang Qi:** Data curation, Methodology. **Wei Terry Chen:** Writing – review & editing. **Yu Shen:** Data curation, Visualization.

Declaration of Competing Interest

The authors declare that they have no known competing financial interests or personal relationships that could have appeared to influence the work reported in this paper.

Data availability

Data will be made available on request.

Acknowledgement

This study was jointly supported by grants from a Major Research Plan of the National Science Foundation of China (92162323, 91962216), the Institute of Geochemistry, Chinese Academy of Science, and China University of Geosciences (Wuhan) to MFZ. We appreciate constructive comments from editors and reviewers.

References

Aiglsperger, T., Proenza, J.A., Lewis, J.F., Labrador, M., Svojtka, M., Rojas-Puron, A., Longo, F., Ďurišová, J., 2016. Critical metals (REE, Sc, PGE) in Ni laterites from Cuba and the Dominican Republic. Ore Geol. Rev. 73, 127–147.

Ali, J.R., Thompson, G.M., Zhou, M.-F., Song, X., 2005. Emeishan large igneous province. SW China: Lithos 79 (3–4), 475–489.

Babechuk, M.G., Widdowson, M., Kamber, B.S., 2014. Quantifying chemical weathering intensity and trace element release from two contrasting basalt profiles. Deccan Traps, India: Chemical Geology 363, 56–75.

Cao, D.B., Chen, K.H., Yin, Y.J., 1993. Characteristics of zoning ultrabasic-basic intrusion in Yuhezhai, Yunnan. Regional Geology of China 1, 28–34.

Chassé, M., Griffin, W.L., O'Reilly, S.Y., Calas, G., 2017. Scandium speciation in a world-class lateritic deposit. Geochem. Perspect. Lett. 3, 105–114.

Chassé, M., Griffin, W.L., O'Reilly, S.Y., Calas, G., 2019. Australian laterites reveal mechanisms governing scandium dynamics in the critical zone. Geochim. Cosmochim. Acta 260, 292–310.

Chung, S.-L., Jahn, B.-M., 1995. Plume-lithosphere interaction in generation of the Emeishan flood basalts at the Permian-Triassic boundary. Geology 23 (10), 889–892.

Dill, H.G., Weber, B., Füssl, M., Melcher, F., 2006. The origin of the hydrous scandium phosphate, kolbeckite, from the Hagendorf-Pleystein pegmatite province, Germany. Mineral. Mag. 70 (3), 281–290.

Duzgoren-Aydin, N.S., Aydin, A., 2003. Chemical heterogeneities of weathered igneous profiles: implications for chemical indices. Environ. Eng. Geosci. 9 (4), 363–377.

Guo, Y.S., Zeng, P.S., Guo, X., Cui, Y.L., Yang, X.S., Lu, W.J., Guo, Q., Yang, Z.L., 2012. Some problems concerning scandium and Scandium-bearing potential of the mafic-ultramafic intrusions in central Yunnan Province. Acta Geol. Sin. 33 (5), 745–754.

Jaireth, S., Hoatson, D.M., Miezitis, Y., 2014. Geological setting and resources of the major rare-earth-element deposits in Australia. Ore Geol. Rev. 62, 72–128.

Ji, H., Wang, S., Ouyang, Z., Zhang, S., Sun, C.X., Liu, X.M., Zhou, D.Q., 2004. Geochemistry of red residua underlying dolomites in karst terrains of Yunnan-Guizhou Plateau: I. The formation of the Pingba profile: Chemical Geology 203 (1–2), 1–27.

Kempe, U., Wolf, D., 2006. Anomalously high Sc contents in ore minerals from Sn–W deposits: possible economic significance and genetic implications. Ore Geol. Rev. 28 (1), 103–122.

Kisakürek, B., Widdowson, M., James, R.H., 2004. Behaviour of Li isotopes during continental weathering: the Bidar laterite profile, India. Chem. Geol. 212, 27–44.

Liu, S., Fan, H.-R., Santosh, M., Liu, X., Wang, Q.-W., Butcher, A.R., 2023. Geological resources of scandium: a review from a Chinese perspective: International Geology Review. https://doi.org/10.1080/00206814.2023.2169842.

Liu, J.P., Wang, X.F., Wang, X.H., Yang, A.P., Song, D.H., Tian, S.M., Xia, C.X., Zhang, K., Yang, S.F., 2020. Charateristics of the late Middle Permian mafic-ultramafic rocks in Dianzhong area, central Yunnan, and their relationship with the Emei Mantle plume. Geology Review 66 (5), 1284–1298.

Ma, Y.X., Ji, X.T., Li, J.C., Huang, M., Min, Z.Z., 2003. Mineral resources of Panzhihua. Chengdu University of Technology, Chengdu, Sichuan Province, SW China, p. 275.

Maulana, A., Sanematsu, K., Sakakibara, M., 2016. An overview on the possibility of scandium and REE occurrence in Sulawesi, Indonesia. Indonesian Journal on Geoscience 3, 139–147.

Mei, H.J., Xu, Y.G., Xu, J.F., Huang, X.L., He, D.C., 2003. Late Permian basalt-phonolite suite from Longzhoushan in the Panxi rift zone. Acta Geological Sinica 77, 341–358.

Orberger, B., van der Ent, A., 2019. Nickel laterites as sources of nickel, cobalt and scandium: increasing resource efficiency through new geochemical and biological insights. J. Geochem. Explor. 204, 297–299.

Putzolu, F., Boni, M., Mondillo, N., Maczurad, M., Pirajno, F., 2019. Ni-Co enrichment and high-tech metals geochemistry in the Wingellina Ni-Co oxide-type laterite deposit (Western Australia). J. Geochem. Explor. 196, 282–296.

Qi, L., Hu, J., Gregoire, D.C., 2000. Determination of trace elements in granites by inductively coupled plasma-mass spectrometry. Talanta 51, 507–513.

Schellmann, W., 1986. A new definition of laterite, In Banerji, P.K., ed., Lateritisation Processes. Memoirs of the Geological Survey of India 120, 1–7.

Shannon, R.D.T., 1976. Revised effective ionic radii and systematic studies of interatomic distances in halides and chalcogenides. Acta Crystallograph. Sect. A: Cryst. Phys. Diffract. Theoret. General Crystallogr. 32 (5), 751–767.

Shellnutt, J.G., Zhou, M.-F., Yan, D.-P., Wang, Y.-B., 2008. Longevity of the Permian Emeishan mantle plume (SW China): 1 Ma, 8 Ma or 18 Ma? Geol. Mag. 145 (3), 373–388.

Shellnutt, J.G., Denyszyn, S.W., Mundil, R., 2012. Precise age determination of mafic and felsic intrusive rocks from the Permian Emeishan large igneous province (SW China). Gondw. Res. 22 (1), 118–126.

Shen, G.F., 2002. Weathering crust of Baihuanao granite: A potential superlarge-scale Rb. Cs, Y, Sc, quartz and albite ore deposit: Bull Miner Petrol Geochem 21, 182–184.

Song, X.-Y., Zhou, M.-F., Cao, Z.-M., Sun, M., Wang, Y.-L., 2003. Ni–Cu–(PGE) magmatic sulfide deposits in the Yangliuping area, Permian Emeishan igneous province, SW China. Miner. Deposita 38 (7), 831–843.

Sun, J., Liu, Y., Liu, X., 2021. Iron Isotope Constraints on the Mineralization Process of Shazi Sc-Rich Laterite Deposit in Qinglong County 11, 737.

Teitler, T., Cathelineau, M., Ulrich, M., Ambrosi, J.P., Munoz, M., Sevin, B., 2019. Petrology and geochemistry of scandium in New Caledonian Ni-Co laterites. J. Geochem. Explor. 196, 131–155.

U.S. Geological Survey, 2021. Mineral commodity summaries 2021. U.S. Geological Survey, St. Louis, p. 200.

Ulrich, M., Cathelineau, M., Munoz, M., Boiron, M.C., Teitler, Y., Karpoff, A.M., 2019. The relative distribution of critical (Sc, REE) and transition metals (Ni Co, Cr, Mn, V) in some Ni-laterite deposits of New Caledonia. J. Geochem. Explor. 197, 93–113.

Voncken, J.H.L., 2016. The Rare Earth Elements: An Introduction. Springer International Publishing.

Wang, Y., Fan, W., Zhang, G., Zhang, Y., 2013. Phanerozoic tectonics of the South China Block: key observations and controversies. Gondw. Res. 23 (4), 1273–1305.

Wang, Z.C., Li, M.Y.H., Liu, Z.-R., Zhou, M.-F., 2021. Scandium: Ore deposits, the pivotal role of magmatic enrichment and future exploration. Ore Geol. Rev. 128, 103906.

Wang, W., Pranolo, Y., Cheng, C.Y., 2011. Metallurgical processes for scandium recovery from various resources: a review. Hydrometall. 108, 100–108.

Wang, Y.B., Wang, D.H., Han, J., Chen, Z.H., Wang, Q.L., 2010. U-Pb dating and Hf isotopic characteristics of zircons from quartz-diorite in the Yijiang REE-Sc deposit, Rucheng County, Hunan: Constraints on the timing of Caledonian magmatic activity in South China: China. Geology 37, 1062–1069.

Wang, C.Y., Zhou, M.-F., Qi, L., 2007. Permian flood basalts and mafic intrusions in the Jinping (SW China)-Song Da (northern Vietnam) district: Mantle sources, crustal contamination and sulfide segregation. Chem. Geol. 243 (3–4), 317–343.

Wang, Z.-C., Zhou, M.-F., Li, M.Y.H., Robinson, P.T., Harlov, D.E., 2022. Kinetic controls on Sc distribution in diopside and geochemical behavior of Sc in magmatic systems. Geochim. Cosmochim. Acta 325, 316–332.

White, A.F., 1995, Chemical weathering rates of silicate minerals soils. In: White, A.F., and Brantley, S.L. (Eds.), Chemical Weathering Rates of Silicate Minerals: Reviews in Mineralogy and Geochemistry, vol. 31, pp. 407–461.

Williams-Jones, A.E., Vasyukova, O.V., 2018. The economic geology of scandium, the runt of the rare earth element litter. Econ. Geol. 113 (4), 973–988.

Xu, Y.-G., He, B., Chung, S.-L., Menzies, M.A., Frey, F.A., 2004. Geologic, geochemical, and geophysical consequences of plume involvement in the Emeishan flood basalt province. Geology 32 (10), 917–920.

Zhao, G.C., Cawood, P.A., 2012. Precambrian geology of China. Precambr. Res. 222–223, 13–54.

Zhao, Z., Wang, D.H., Chen, Z.H., Zheng, G.D., 2012. Supergene enrichment pattern of Sc in weathering crust of the Zhaibei granite. Nanling region: Miner Depos 31, 1217–1218.

Zhong, H., Qi, L., Hu, R.-Z., Zhou, M.-F., Gou, T.-Z., Zhu, W.-G., Liu, B.-G., Chu, Z.-Y., 2011. Rhenium-osmium isotope and platinum-group elements in the Xinjie layered intrusion, SW China: Implications for source mantle composition, mantle evolution, PGE fractionation and mineralization. Geochim. Cosmochim. Acta 75 (6), 1621–1641.

Zhou, M.-F., Malpas, J., Song, X.-Y., Robinson, P.T., Sun, M., Kennedy, A.K., Lesher, C.M., Keays, R.R., 2002b. A temporal link between the Emeishan large igneous province (SW China) and the end-Guadalupian mass extinction. Earth Planet. Sci. Lett. 196 (3–4), 113–122.

Zhou, M.F., Yan, D.P., Kennedy, A.K., Li, Y.Q., Ding, J., 2002a. SHRIMP zircon geochronological and geochemical evidence for Neo-proterozoic arc-related magmatism along the western margin of the Yangtze Block. South China: Earth Planet. Sci. Lett. 196, 51–67.

Zhou, M.F., Robinson, P.T., Lesher, C.M., Keays, R.R., Zhang, C.-J., Malpas, J., 2005. Geochemistry, Petrogenesis and Metallogenesis of the Panzhihua Gabbroic Layered

Intrusion and Associated Fe-Ti-V Oxide Deposits, Sichuan Province, SW China. J. Petrol. 46 (11), 2253–2280.
Zhou, M.F., Li, X.X., Wang, Z.C., Li, X.C., Liu, J.C., 2020. The genesis of regolith-hosted rare earth element and scandium deposits: Current understanding and outlook to future prospecting. Chin. Sci. Bull. 65, 3809–3824.
Zhou, M.-F., Wang, Z.-C., Zhao, W.W., Qi, L., Zhao, Z., Zhou, J., Huang, Z., Chen, W.T., 2022. A reconnaissance study of potentially important scandium deposits associated with carbonatite and alkaline igneous complexes of the Permian Emeishan Large Igneous Province. SW China: J. Asian Earth Sci. 236, 105309.
Zhu, Z.H., 2010. The discovery and significance of Sc in the Ertaipo rock body of Mouding. Yunnan: Yunnan Geol. 29 (3), 235–244.